Conjugated Oligomers

DOI: 10.1002/anie.201000555

A Modular Synthetic Approach to Conjugated Pentacene Di-, Tri-, and Tetramers**

*Dan Lehnherr, Adrian H. Murray, Robert McDonald, and Rik R. Tykwinski**

Pentacene and functionalized pentacenes are leading candidates for small-molecule semiconductor applications and have been widely explored over the past decade.[1] On the other hand, examples of pentacene polymers[2,3a–c] and oligomers[3] remain scarce, even though they present obvious opportunities for discovery. In comparison to polymers, monodisperse oligomers provide the added benefit of structural homogeneity. Furthermore, oligomers allow for the systematic study of structure–property relationships, in which a property of interest (e.g., HOMO–LUMO gap (HOMO = highest occupied molecular orbital, LUMO = lowest unoccupied molecular orbital)) is examined as a function of oligomer length. If oligomers of sufficient length are accessible, the effective conjugation length can be determined by observing saturation of a property; that is, when the oligomer starts to behave like the polymer.[4]

To date, the synthesis of functionalized pentacenes has relied, to a large extent, on the addition of nucleophiles to acenequinones such as 6,13-pentacenequinone, followed by reduction to form the aromatic pentacene framework.[1] This methodology cannot, however, easily be adapted to the synthesis of conjugated oligomers.[3d] Such synthetic limitations are due, in part, to the reactive nature of the pentacene core and to the limits of current methodology for desymmetrizing the pentacene chromophore. It is unlikely that this issue can be effectively addressed by condensation[5a] and cycloaddition[5b–f] reactions to form acenes, since such methods often produce isomeric mixtures. Oxidative acetylenic homo- and cross-coupling reactions of terminal and/or haloacetylenes (e.g., Hay and Cadiot–Chodkiewicz reactions) are a well-established means of assembling carbon-rich materials.[6] These reactions, when paired with recently developed methods to form unsymmetrical pentacenes,[7] would serve as the foundation for the synthesis of a homologous series of pentacene oligomers.

Pentacenes that bear a terminal acetylene functionality, such as **1** or **2** (Scheme 1), are quite reactive,[7a] and have been ineffective to date when isolated and used as precursors for synthetic elaboration.[8] To circumvent this problem, a protection method has been developed[9] so that the synthetic potential of terminal acetylenes can be accommodated and exploited. Herein, we report the synthesis of protected building blocks such as **3** and **4**, and describe their application to metal-mediated coupling reactions used in the synthesis of a series of conjugated pentacene oligomers (**5**–**8**, Scheme 2). The properties of these oligomers are explored by crystallographic, spectroscopic, and electrochemical methods.

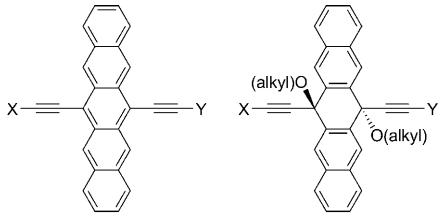

1 X = Si(*i*Pr)$_3$, Y = H
2 X = Y = H
3 X = Si(alkyl)$_3$, Y = H or Br
4 X = Y = H or Br

Scheme 1. Structures of pentacenes **1**–**4**.

The construction of pentacene oligomers **6**–**8** begins with desymmetrizing 6,13-pentacenequinone (**9**, Scheme 3). Addition of one equivalent of the appropriate lithium acetylide (**10a**–**d**) to a suspension of **9** in THF afforded monoaddition products **11a**–**d** in good yields (80–96%). Addition of an excess of acetylide **10e** (ca. 3 equiv) to ketones **11a**–**d**, followed by trapping of the resulting alkoxide with iodomethane afforded methyl ethers **12a**–**d** in good yield (69–79%). Methyl ether **12e**, which bears two $Me_3Si{-}C{\equiv}C$ groups was obtained directly from quinone **9** in 57% yield. Protodesilylation of the Me_3Si group(s) of **12a**–**e** provided **13a**–**e** in 88–99% yield. Terminal acetylenes **13c** and **13e** were then converted to bromoalkynes **14c** and **14e** using the standard conditions of *N*-bromosuccinimide (NBS) and $AgNO_3$ in acetone.[10] The *trans* geometry of the methyl ethers for a number of derivatives (**12a**–**b**, **13a**–**b**, **13d**, **14e**) was confirmed by X-ray crystallography, and the stereochemistry of related structures was assigned by analogy.[11]

[*] D. Lehnherr, A. H. Murray, Prof. Dr. R. R. Tykwinski[+]
Department of Chemistry, University of Alberta
Edmonton, Alberta, T6G 2G2 (Canada)
Fax: (+1) 780-492-8231
E-mail: rik.tykwinski@chemie.uni.erlangen.de
Dr. R. McDonald
X-ray Crystallography Laboratory, Department of Chemistry
University of Alberta
Edmonton, Alberta, T6G 2G2 (Canada)
[+] Present address: Institut für Organische Chemie
Friedrich-Alexander-Universität, Erlangen-Nürnberg
Henkestrasse 42, 91054 Erlangen (Germany)

[**] This work was generously supported by the University of Alberta, the Natural Sciences and Engineering Research Council of Canada (NSERC) through the Discovery grant program, and the Canadian Foundation for Innovation (CFI). D.L. thanks NSERC (PGS-D), the Alberta Ingenuity Fund (AIF) , the Alberta Heritage Fund, the Killam Trusts, and the University of Alberta for scholarship support. A.H.M. thanks NSERC (PGS-D) and AIF for scholarship support.
Supporting information for this article is available on the WWW under http://dx.doi.org/10.1002/anie.201000555.

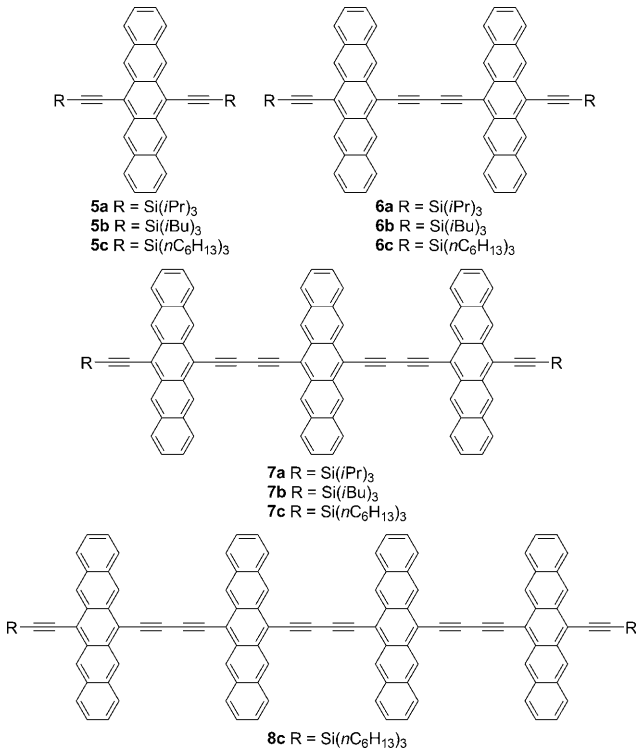

Scheme 2. Structures of monomeric pentacenes **5a–c** and the homologous conjugated pentacene oligomers **6–8**.

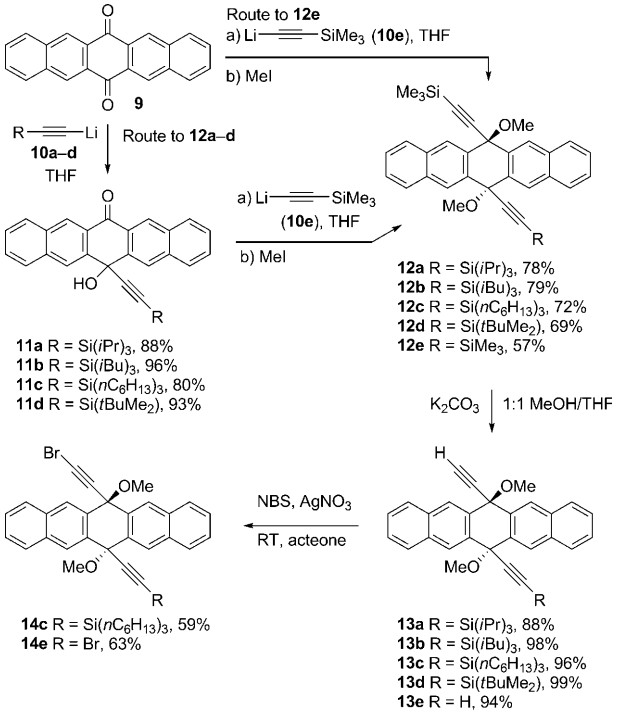

Scheme 3. Synthesis of pentacene building blocks **13** and **14**.

Hay homocoupling[12] of building blocks **13a–d** afforded **15a–d** in 56–64% yield,[13] and Sn^{II}-mediated reductive aromatization afforded conjugated dimers **6a–c** in excellent yields (Scheme 4). Although the reduction of related diols and tetraols has been accomplished without the use of

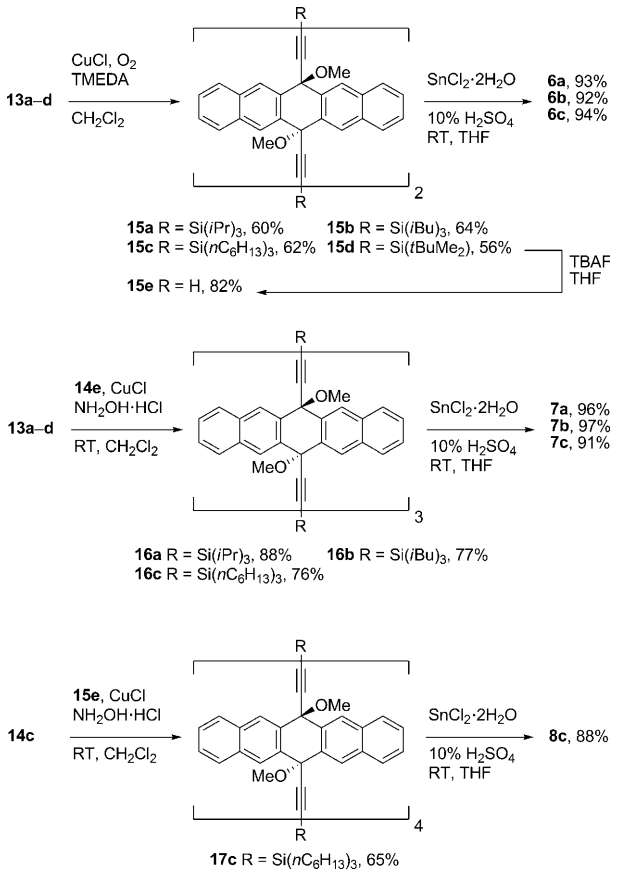

Scheme 4. Synthesis of conjugated pentacene oligomers **6–8**. TBAF = tetrabutylammonium fluoride; TMEDA = *N*,*N*,*N*′,*N*′-tetramethylethylenediamine

additional acid,[3,7] aromatization of **15a–c** did not proceed at an appreciable rate in the absence of H_2SO_4.

Cadiot–Chodkiewicz[14] coupling of the appropriate terminal alkyne **13a–d** with bromoalkyne **14e** provided **16a–c** in 76–88% yield (Scheme 4). Reductive aromatization of **16a–c** then gave pentacene trimers **7a–c** in excellent yields. The synthesis of pentacene tetramer **8c** (Scheme 4) began with the removal of the *tert*-butyldimethylsilyl (TBS) groups of dimeric dihydropentacene **15d** with TBAF to provide **15e**,[15] the stereochemistry of which was confirmed by X-ray crystallography.[11] Cadiot–Chodkiewicz coupling of **15e** with bromoalkyne **14c** provided **17c** in 65% yield. Compound **17c** was then aromatized to form the pentacene tetramer **8c** in excellent yield.

A major consideration for essentially planar π systems is solubility, and all three monomers **5a–c**[16] are highly soluble in common organic solvents such as CH_2Cl_2, $CHCl_3$, THF, and toluene. The $Si(iPr)_3$-substituted dimer **6a** has, unfortunately, limited solubility in these solvents ($< 5\ mg\,mL^{-1}$). The larger iBu_3Si group resulted in improved solubility for dimer **6b** compared to **6a**, but proved ineffective for solubilizing the trimer **7b**. Trimer **7c** has good solubility as a result of the $Si(nC_6H_{13})_3$ groups. On the other hand, tetramer **8c** shows disappointingly poor solubility in THF, and even worse solubility in CH_2Cl_2 or $CHCl_3$.

The choice of the trialkylsilyl group affects not only the solubility but also the stability of the oligomer, as can be observed by differential scanning calorimetry (DSC) analysis (Table 1). The decomposition temperatures of the oligomers generally decrease as the steric bulk around the silyl group is reduced. Thus, in all cases, the Si(*i*Pr)$_3$ derivatives (**5a**–**7a**) show the highest stability, while the Si(nC$_6$H$_{13}$)$_3$ analogues are the least stable. Additionally, when oligomers with identical end groups are compared, the stability increases as a function of the number of repeat units in the oligomer. This trend is illustrated with the Si(nC$_6$H$_{13}$)$_3$ series, where the decomposition temperature increases from monomer **5c** (130 °C), to dimer **6c** (134 °C), to trimer **7c** (162 °C), and tetramer **8c** (250 °C).

Table 1: Optical and thermal properties of pentacenes **5**–**8**.

Cmpd	λ_{max} (THF) [nm]	λ_{max} (CH_2Cl_2) [nm]	λ_{max}[a] (film) [nm]	λ_{max}[b] (film) [nm]	E_g^{opt}[c] (THF) [eV]	T_d[d] (TGA/DSC) [°C]
5a	641	643	702	696	1.86	375/263
5b	642	644	667	667	1.86	360/213
5c	641	644	713	703	1.86	485/130
6a	736	739	858	784	1.57	410/365
6b	738	740	778	776	1.59	375/267
6c	737	739	872	836	1.57	375/134
7a	–	–	–	–	–	400/350
7b	–	–	–	–	–	350/270
7c	801[e]	797[e]	964	–	1.39	390/162
8c	815[e]	–	–	–	< 1.38	385/250

[a] Thin film formed by drop-casting from THF (see the Supporting Information for spectra). [b] Thin film formed by drop-casting from $CHCl_3$ (see the Supporting Information for spectra). [c] See reference [17]. [d] Onset decomposition temperatures measured under nitrogen. [e] Estimated λ_{max} value of lowest-energy shoulder signal.

The UV/Vis absorption properties of the oligomeric pentacenes in both THF and CH_2Cl_2 solutions were examined. The solubility of the dimers is slightly better in THF than CH_2Cl_2, although the choice of solvent has little effect on the λ_{max} values (Table 1). The constitution of the pendent trialkylsilyl group also has little effect on the UV/Vis spectra in either the monomer or dimer series **5a**–**c** and **6a**–**c**, respectively. As the oligomer length is increased, a concurrent red shift in the λ_{max} values is observed (Figure 1), and is indicative of increased conjugation. This bathochromic shift in λ_{max} (THF) is most dramatic in the comparison of monomer **5c** to dimer **6c** (96 nm), and diminishes thereafter: compare dimer **6c** with trimer **7c** (64 nm) and trimer **7c** with tetramer **8c** (14 nm). Thus, already by the stage of the tetramer, the effective conjugation length for this series of molecules is nearly achieved. The HOMO–LUMO gap is estimated from the absorption onset (E_g^{opt}),[17] and drops from 1.86 eV (**5c**) to 1.57 eV (**6c**) to approximately 1.38 eV for both **7c** and **8c**. The conjugated oligomers **5c**–**8c** linked at the 6,13 positions therefore possess significantly smaller optical band gaps than the regio-irregular copolymers based on 6,13-bis(triisopropylsilylethynyl)pentacene linked at the 2,9 and/or 2,10 positions (E_g^{opt} = ca. 1.68–1.76 eV).[2b,c] It can be noted that trimer **7c** and tetramer **8c** possess a remarkably low band gap for a material composed of only hydrocarbon chromophores, and these oligomers are comparable to ethynylated heptacenes (ca. 1.3–1.4 eV), some of the lowest band-gap carbon materials reported to date.[18]

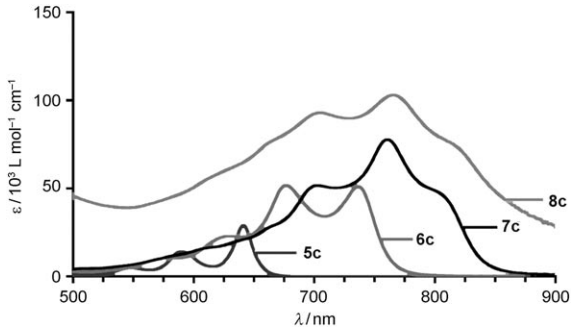

Figure 1. UV/Vis absorption spectra of the homologous series of oligomers **5c**–**8c** in THF solutions (data for **8c** is plotted with arbitrary intensity because of limited solubility).

The emission properties of pentacenes **5**–**8** were studied in CH_2Cl_2 solutions. Monomers **5a**–**c** all emit at 649 nm with a relatively small Stokes shift (ca. 120 cm^{-1}) and $\Phi_F \approx 0.15$.[19] Conjugated oligomers **6c**–**8c** are essentially non-emissive, analogous to previously reported conjugated pentacene dimers.[3d]

Analysis of solid-state UV/Vis absorption was attempted on films drop-cast from THF and $CHCl_3$. In all cases, a bathochromic shift in λ_{max} values was found for thin-film samples compared to those in solution. This effect is most dramatic for films of **5c**, **6c**, and **7c** (molecules terminated with Si(nC$_6$H$_{13}$)$_3$ groups) cast from THF, for which λ_{max} is red-shifted by 72, 135, and 163 nm, respectively. Conversely, the difference between solution- and solid-state λ_{max} values is significantly less for molecules terminated with Si(*i*Bu)$_3$ groups (**5b** and **6b**), thus suggesting that the constitution of the end group exerts an appreciable influence on the solid-state morphology. In comparison to films cast from THF, λ_{max} values observed for those cast from $CHCl_3$ are noticeably blue-shifted (with the exception of **6b**). Thus, not unexpectedly, the solvent used for casting also influences the film morphology.

Cyclic voltammetry was used to examine the solution-state redox properties as a function of oligomer length, although the poor solubility of tetramer **8c** prevented its electrochemical study (Table 2; all potentials are given versus the ferrocene/ferrocenium couple).[20] The first reduction and oxidation events both show a marked dependence on oligomer length. For example, within the series **5c**–**7c**, the first oxidation potential decreases from 0.54 V for **5c** to just 0.33 V for **7c** (the oxidation of trimer **7c** is irreversible and was estimated from the anodic potential E_{pa} of the oxidation wave).

The reduction potentials show an analogous trend, and decrease from −1.49 V for monomer **5c** to −1.13 V for trimer **7c**. A total of two one-electron reductions per pentacene moiety is apparent for each oligomer in the series, that is, monomer **5c**, dimer **6c**, and trimer **7c** each show two, four, and six reductions, respectively. The separation between the first two reduction potentials for dimer **6c** (−1.25 and

Table 2: Electrochemical properties of pentacenes **5**–**7**.[a]

Cmpd	$E_g^{electro}$ [eV]	E_{red1} [V]	E_{red2} [V]	E_{red3} [V]	E_{red4} [V]	E_{ox1} [V]
5a	2.02	−1.48	−1.98	–	–	0.54
5b	2.02	−1.49	−1.97	–	–	0.53
5c	2.03	−1.49	−1.97	–	–	0.54
6c	1.64	−1.25	−1.46	−1.96	−2.19	0.39
7c	1.46	−1.13	−1.25	−1.56	−1.90	0.33[b]

[a] Cyclic voltammetry was performed in THF solutions containing 0.1 M nBu$_4$NPF$_6$ as supporting electrolyte at a scan rate of 150 mVs^{-1}. The potential values (E) were calculated using the following equation (except where otherwise noted): $E = (E_{pc} + E_{pa})/2$, where E_{pc} and E_{pa} correspond to the cathodic and anodic peak potentials, respectively. Potentials are referenced to the ferrocene/ferrocenium (Fc/Fc$^+$) couple used as an internal standard. All potentials represent a one-electron reduction or oxidation event. See reference [20]. [b] This oxidation potential was estimated by reporting the E_{pa} value of the oxidation wave.

−1.46 V) and the first three potentials for trimer **7c** (−1.13, −1.25, and −1.56 V) confirms the electronic communication between pentacene units, which is consistent with the significant decrease in λ_{max} values upon chain elongation (see below). It is also worth noting that, following the formal addition of one electron to each pentacene unit of **5c**–**7c**, the reduction potentials for adding a second electron to a pentacene moiety all occur at a similar potential, regardless of oligomer length, that is, E_{red2} for monomer **5c** (−1.97 V) versus E_{red3} for dimer **6c** (−1.96 V) versus E_{red4} for trimer **7c** (−1.90 V). Finally, the electrochemically determined band gap ($E_g^{electro}$) decreases as a function of the number of repeat units (Table 2), and the $E_g^{electro}$ values are comparable to the E_g^{opt} values determined from the UV/Vis spectroscopic data (Table 1).

A single crystal of dimer **6b** suitable for X-ray crystallographic analysis was obtained from a solution of **6b** in $CHCl_3$ by slow evaporation at 4 °C (to give **6b**·2 $CHCl_3$).[21] The solid-state geometry reveals that the two pentacene moieties of **6b** adopt a pseudocoplanar arrangement in which the packing features a 2D slipped stacked arrangement (Figure 2a). Molecules of **6b** thus form a staircase arrangement along the crystallographic *b* axis, with an interplanar spacing of 3.40 Å between cofacial, π-stacking pentacene moieties (interaction X in Figure 2a). Furthermore, there is minimal slippage along the long axis of the acene moiety (approximately half a benzene ring, see Figure 2b).[22,23] Cofacial π stacking not only occurs within the staircase arrangement along the *b* axis, but also between adjacent staircases along the crystallographic *a* axis (interaction Y in Figure 2a) with an interplanar distance of 3.36 Å and an overlap of approximately 1.5 benzene rings (Figure 2b).[22] This 2D slipped-stack arrangement, together with the ability of the butadiynyl to facilitate electronic communication, provides the potential for 3D electronic communication in the solid state, and could greatly simplify device formation.[24,25]

In summary, a new synthetic methodology allows for the use of acetylenic coupling methods for the construction of conjugated pentacene oligomers. Reduction of the optical band gap is observed as a function of the oligomer length, and the conjugated pentacene tetramer **8c** shows an E_g^{opt} value less than 1.4 eV. The UV/Vis spectra suggest that the effective conjugation length attainable for this series of oligomers has been nearly reached by the stage of the tetramer. The application of this methodology to other oligoacenes and the incorporation of solubilizing groups into the repeat unit are in progress.

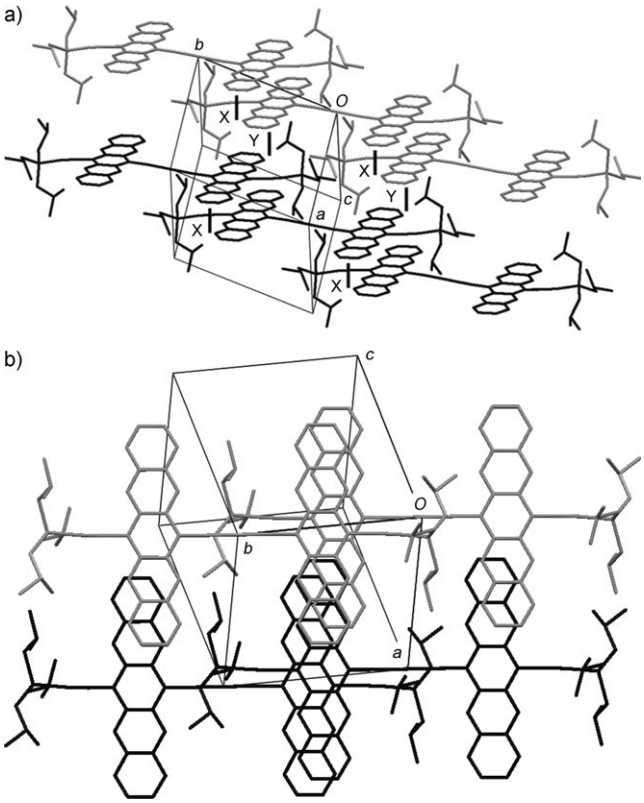

Figure 2. X-ray crystallographic structure of dimer **6b**·2 $CHCl_3$ illustrating a) the interaction of neighboring pentacene dimers in the staircase along the crystallographic *b* axis (labeled X) and of two adjacent staircases along the crystallographic *a* axis (labeled Y). b) Effective overlap of pentacene moieties as viewed from above. $CHCl_3$ molecules and hydrogen atoms have been omitted for clarity.

Received: January 30, 2010
Revised: April 29, 2010
Published online: July 19, 2010

Keywords: acenes · C—C coupling · oligomerization · π interactions · semiconductors

[1] a) J. E. Anthony, *Chem. Rev.* **2006**, *106*, 5028–5048; b) J. E. Anthony, *Angew. Chem.* **2008**, *120*, 460–492; *Angew. Chem. Int. Ed.* **2008**, *47*, 452–483.
[2] a) S. Tokito, K.-H. Weinfurtner, H. Fujikawa, T. Tsutsui, Y. Taga, *Proc. SPIE-Int. Soc. Opt. Eng.* **2001**, *4105*, 69–74; b) T. Okamoto, Z. Bao, *J. Am. Chem. Soc.* **2007**, *129*, 10308–10309; c) T. Okamoto, Y. Jiang, F. Qu, A. C. Mayer, J. E. Parmer, M. D. McGehee, Z. Bao, *Macromolecules* **2008**, *41*, 6977–6980.
[3] a) D. Lehnherr, R. R. Tykwinski, *Materials* **2010**, *3*, 2772–2800; b) D. Lehnherr, R. R. Tykwinski, *Org. Lett.* **2007**, *9*, 4583–4586; c) D. Lehnherr, R. McDonald, M. J. Ferguson, R. R. Tykwinski, *Tetrahedron* **2008**, *64*, 11449–11461; d) D. Lehnherr, J. Gao, F. A. Hegmann, R. R. Tykwinski, *Org. Lett.* **2008**, *10*, 4779–

4782; e) D. Lehnherr, J. Gao, F. A. Hegmann, R. R. Tykwinski, *J. Org. Chem.* **2009**, *74*, 5017 – 5024; f) X. Zhang, X. Jiang, J. Luo, C. Chi, H. Chen, J. Wu, *Chem. Eur. J.* **2010**, *16*, 464 – 468.

[4] a) H. Meier, *Angew. Chem.* **2005**, *117*, 2536 – 2561; *Angew. Chem. Int. Ed.* **2005**, *44*, 2482 – 2506; b) R. E. Martin, F. Diederich, *Angew. Chem.* **1999**, *111*, 1440 – 1469; *Angew. Chem. Int. Ed.* **1999**, *38*, 1350 – 1377; c) *Electronic Materials — The Oligomer Approach* (Eds.: K. Müllen, G. Wegner), Wiley-VCH, Weinheim, **1998**.

[5] For representative synthetic methods to the pentacene framework, see: a) M. M. Payne, S. A. Odom, S. R. Parkin, J. E. Anthony, *Org. Lett.* **2004**, *6*, 3325 – 3328; b) T. Takahashi, M. Kitamura, B. Shen, K. Nakjima, *J. Am. Chem. Soc.* **2000**, *122*, 12876 – 12877; c) J. Lu, D. M. Ho, N. J. Vogelaar, C. M. Kraml, S. Bernhard, N. Byrne, L. R. Kim, R. A. Pascal, Jr., *J. Am. Chem. Soc.* **2006**, *128*, 17043 – 17050; d) Q. Miao, X. Chi, S. Xiao, R. Zeis, M. Lefenfeld, T. Siegrist, M. L. Steigerwald, C. Nuckolls, *J. Am. Chem. Soc.* **2006**, *128*, 1340 – 1345; e) J. E. Rainbolt, G. P. Miller, *J. Org. Chem.* **2007**, *72*, 3020 – 3030; f) Y. Zhao, R. Mondal, D. C. Neckers, *J. Org. Chem.* **2008**, *73*, 5506 – 5513.

[6] a) *Carbon-Rich Compounds* (Eds.: M. M. Haley, R. R. Tykwinski), Wiley-VCH, Weinheim, **2006**; b) *Acetylene Chemistry: Chemistry, Biology, and Material Science* (Eds.: F. Diederich, P. J. Stang, R. R. Tykwinski), Wiley-VCH, Weinheim, **2005**; c) P. Siemsen, R. C. Livingston, F. Diederich, *Angew. Chem.* **2000**, *112*, 2740 – 2767; *Angew. Chem. Int. Ed.* **2000**, *39*, 2632 – 2657.

[7] a) D. Lehnherr, R. McDonald, R. R. Tykwinski, *Org. Lett.* **2008**, *10*, 4163 – 4166; b) D. Lehnherr, A. H. Murray, R. McDonald, M. J. Ferguson, R. R. Tykwinski, *Chem. Eur. J.* **2009**, *15*, 12580 – 12584.

[8] In situ generation and derivatization of precursor **2** has been, to the best of our knowledge, successful in two cases, see: a) K. Susumu, T. V. Duncan, M. J. Therien, *J. Am. Chem. Soc.* **2005**, *127*, 5186 – 5195; b) C.-Y. Lin, Y.-C. Wang, S.-J. Hsu, C.-F. Lo, E. W.-G. Diau, *J. Phys. Chem. C* **2010**, *114*, 687 – 693.

[9] For the elegant use of a similar protection method for the formation of anthracene polymers, see: M. S. Taylor, T. M. Swager, *Angew. Chem.* **2007**, *119*, 8632 – 8635; *Angew. Chem. Int. Ed.* **2007**, *46*, 8480 – 8483.

[10] H. Hofmeister, K. Annen, H. Laurent, R. Wiechert, *Angew. Chem.* **1984**, *96*, 720 – 722; *Angew. Chem. Int. Ed. Engl.* **1984**, *23*, 727 – 729.

[11] See the Supporting Information for X-ray crystallographic structures and details. CCDC- 760494 (**12a**), 760495 (**12b**), 760496 (**13a**), 760497 (**13b**), 760498 (**13d**), 760499 (**14e**), 760500 (**15e**) contain the supplementary crystallographic data for these compounds. These data can be obtained free of charge from The Cambridge Crystallographic Data Centre via www.ccdc.cam.ac.uk/data_request/cif.

[12] A. S. Hay, *J. Org. Chem.* **1962**, *27*, 3320 – 3321.

[13] Unprotected analogues to **13a** that contain two hydroxy moieties were found to be unsuitable for metal-mediated coupling reactions such as those presented herein, see reference [7a].

[14] W. Chodkiewicz, *Ann. Chim. (Paris)* **1957**, *2*, 819 – 869.

[15] Desilylation of **15d** with CsF in 5:1 THF/H_2O, or KF in 5:1 THF/H_2O resulted in recovery of the starting material.

[16] Monomers **5a–c** were synthesized by addition of the corresponding lithium acetylide to 6,13-pentacenequinone followed by treatment of the resulting diol with $SnCl_2{\cdot}2H_2O$. See the Supporting Information for details.

[17] The value used as the absorption edge corresponds to the lowest-energy absorption wavelength with a molar absorptivity (ε) $\geq 1000\ L\,mol^{-1}\,cm^{-1}$.

[18] a) S. S. Zade, M. Bendikov, *Angew. Chem.* **2010**, *122*, 4104 – 4107; *Angew. Chem. Int. Ed.* **2010**, *49*, 4012 – 4015; b) M. M. Payne, S. R. Parkin, J. E. Anthony, *J. Am. Chem. Soc.* **2005**, *127*, 8028 – 8029; c) D. Chun, Y. Cheng, F. Wudl, *Angew. Chem.* **2008**, *120*, 8508 – 8513; *Angew. Chem. Int. Ed.* **2008**, *47*, 8380 – 8385.

[19] Fluorescence quantum efficiencies were obtained relative to cresyl violet perchlorate in methanol, see: S. J. Isak, E. M. Eyring, *J. Phys. Chem.* **1992**, *96*, 1738 – 1742.

[20] See the Supporting Information for cyclic voltammograms and a complete table of redox potentials in CH_2Cl_2 and THF.

[21] X-ray data for **6b**·2 $CHCl_3$: $C_{78}H_{80}Cl_6Si_2$, $M_r = 1286.30$; crystal dimensions (mm) $0.54 \times 0.44 \times 0.08$; triclinic space group $P\bar{1}$ (No. 2); $a = 10.1229(10)$, $b = 11.4926(11)$, $c = 15.3308(15)$ Å; $\alpha = 101.5627(12)$, $\beta = 91.9451(12)$, $\gamma = 96.5342(12)°$; $V = 1733.1(3)$ Å^3; $Z = 1$; $\rho_{calcd} = 1.232\ g\,cm^{-3}$; $\mu = 0.325\ mm^{-1}$; $\lambda = 0.71073$ Å; $T = -100\,°C$; $2\theta_{max} = 51.52°$; total data collected = 12984; $R_1 = 0.0695$ [5119 observed reflections with $F_o^2 \geq 2\sigma(F_o^2)$]; $wR_2 = 0.2102$ for 439 variables, 13 restraints, and 6603 unique reflections; residual electron density = 0.720 and $-0.552\ e\,Å^{-3}$. The C(34A)–C(35A) and C(34B)–C(35B) distances (within a partially disordered silyl isobutyl group) were constrained to be equal (within 0.01 Å) during refinement. The Cl–C distances (Cl(1S)–C(1S), Cl(2S)–C(1S), Cl(1S)–C(3S), Cl(4S)–C(2S), Cl(5S)–C(2S), Cl(6S)–C(2S) within the disordered solvent chloroform molecule were constrained to be equal (within 0.03 Å) to a common value, as were the Cl–Cl distances [Cl(1S)–Cl(2S), Cl(1S)–Cl(3S), Cl(2S)–Cl(3S), Cl(4S)–Cl(5S), Cl(4S)–Cl(6S), Cl(5S)–Cl(6S). CCDC- 760493 contains the supplementary crystallographic data for this compound. These data can be obtained free of charge from The Cambridge Crystallographic Data Centre via www.ccdc.cam.ac.uk/data_request/cif.)

[22] Interplanar distances were calculated from the distance between the least-squares plane generated from the acene carbon atoms of one pentacene moiety and that of its noncovalent neighboring moiety.

[23] For a related crystal structure of a conjugated anthracene–pentacene dyad, see reference [7b].

[24] H. Pang, F. Vilela, P. J. Skabara, J. J. W. McDouall, D. J. Crouch, T. D. Anthopoulos, D. D. C. Bradley, D. M. de Leeuw, P. N. Horton, M. B. Hursthouse, *Adv. Mater.* **2007**, *19*, 4438 – 4442.

[25] While red-shifted λ_{max} values for **6b** are qualitatively consistent with π stacking observed in the crystallographic analysis, more definitive conclusions are tenuous without additional data regarding the morphology of crystals of **6b** grown from THF or knowledge of the film morphology used for the UV/Vis analyses. Crystals of **6b** were grown from THF/MeOH and CH_2Cl_2 solutions, but unfortunately, neither data set was suitable for publication.

